Biochimica et Biophysica Acta 1808 (2011) 78–90

Contents lists available at ScienceDirect

Biochimica et Biophysica Acta

journal homepage: www.elsevier.com/locate/bbamem

Characterization of superoxide overproduction by the D-Loop$_{Nox4}$-Nox2 cytochrome b_{558} in phagocytes—Differential sensitivity to calcium and phosphorylation events

Laure Carrichon [a], Antoine Picciocchi [a], Franck Debeurme [a], Federica Defendi [a], Sylvain Beaumel [a], Algirdas J. Jesaitis [b], Marie-Claire Dagher [a], Marie-José Stasia [a,*]

[a] Centre Diagnostic et Recherche sur la Granulomatose septique chronique CGD, TheREx-TIMC/Imag UMR CNRS 5525, CHU and Université Joseph Fourier, 38043 Grenoble Cedex 9, France
[b] Department of Microbiology, 109 Lewis Hall, Montana State University, Bozeman, MT 59717, USA

ARTICLE INFO

Article history:
Received 30 March 2010
Received in revised form 2 August 2010
Accepted 3 August 2010
Available online 11 August 2010

Keywords:
NADPH oxidase
Activation
ROS overproduction
Microbicidy
PLB-985 cells
Neutrophils

ABSTRACT

NADPH oxidase is a crucial element of phagocytes involved in microbicidal mechanisms. It becomes active when membrane-bound cytochrome b_{558}, the redox core, is assembled with cytosolic p47^{phox}, p67^{phox}, p40^{phox}, and *rac* proteins to produce superoxide, the precursor for generation of toxic reactive oxygen species. In a previous study, we demonstrated that the potential second intracellular loop of Nox2 was essential to maintaining NADPH oxidase activity by controlling electron transfer from FAD to O_2. Moreover, replacement of this loop by the Nox4-D-loop (D-loop$_{Nox4}$-Nox2) in PLB-985 cells induced superoxide overproduction. In the present investigation, we demonstrated that both soluble and particulate stimuli were able to induce this superoxide overproduction. Superoxide overproduction was also observed after phosphatidic acid activation in a purified cell-free-system assay. The highest oxidase activity was obtained after ionomycin and fMLF stimulation. In addition, enhanced sensitivity to Ca^{2+} influx was shown by thapsigargin, EDTA, or BTP2 treatment before fMLF activation. Mutated cytochrome b_{558} was less dependent on phosphorylation triggered by ERK1/2 during fMLF or PMA stimulation and by PI3K during OpZ stimulation. The superoxide overproduction of the D-loop$_{Nox4}$-Nox2 mutant may come from a change of responsiveness to intracellular Ca^{2+} level and to phosphorylation events during oxidase activation. Finally the D-loop$_{Nox4}$-Nox2-PLB-985 cells were more effective against an attenuated strain of *Pseudomonas aeruginosa* compared to WT-Nox2 cells. The killing mechanism was biphasic, an early step of ROS production that was directly bactericidal, and a second oxidase-independent step related to the amount of ROS produced in the first step.

1. Introduction

Polymorphonuclear neutrophils play a key role in host defenses against intrusive microorganisms and have a major function in inflammation. Indeed, in response to a variety of agents, neutrophils release large quantities of superoxide anions ($O_2^{\cdot-}$) and other reactive oxygen species (ROS) in a phenomenon known as the respiratory burst. The NADPH oxidase complex of phagocytes is responsible for $O_2^{\cdot-}$ production [1]. The central importance of the phagocyte NADPH oxidase to innate host defense is illustrated in chronic granulomatous disease (CGD), a rare genetic disorder characterized by severe and recurrent infections due to the inability of phagocytes to produce ROS to kill invading bacteria and fungi. CGD arises from mutations in one of the *CYBB*, *NCF1*, *NCF2*, and *CYBA* genes encoding Nox2, p47^{phox}, p67^{phox}, and p22^{phox} proteins, respectively [2]. NADPH oxidase is a multicomponent enzyme composed of a membrane-bound flavocytochrome b_{558} (cyt b_{558}), cytosolic proteins p67^{phox}, p47^{phox}, p40^{phox}, and two small GTP-binding proteins and Rac1/2. Cyt b_{558}, the catalytic core that transfers electrons from cytosolic NADPH across the plasma membrane to a phagolysosomal or an extracellular O_2, consists of a heavily glycosylated large β subunit (gp91^{phox} or Nox2) and a small α subunit (p22^{phox}) [3]. Hydropathy plots and sequence alignment of Nox2 with members of the ferredoxin-NADP$^+$ reductase family demonstrate the presence of six transmembrane α-helices in the N-terminal hydrophobic region, cytosolic regions: the ^{1}MGNWVAVNEGL^{11}sequence, the B loop ^{70}PVCRNLLSFLRGSSACCSTRIRRQLDRNLTFHK^{102}, the D loop ^{191}TSSTKTIRRS^{200}, and a C-terminal region containing binding sites for FAD and NADPH [4–6]. Recently, two families of Nox homologs, Nox (for *N*ADPH *ox*idase) and Duox (for *du*al *ox*idase), expressed in several tissues and cells and involved in different pathological processes, have been identified. They can generate low amounts of $O_2^{\cdot-}$ and are suggested to be involved in cell signaling, host defense and hypoxia

Abbreviations: ROS, reactive oxygen species; CGD, chronic granulomatous disease; PMA, phorbol 12-myristate 13-acetate; fMLF, formyl-methyl-leucyl-phenylalanine; DMF, dimethylformamide; DFP, diisopropylfluorophosphate; SOD, mAb, monoclonal antibody; cyt b_{558}, cytochrome b_{558}; WT, wild

* Corresponding author. Centre Diagnostic et Recherche sur la granulomatose septique CGD, TheREx-TIMC/Imag UMR CNRS 5525, CHU Grenoble 38043 Grenoble Cedex 9, France. Tel.: +33 476765483; fax: +33 4 76765608.
E-mail address: mjstasia@chu-grenoble.fr (M.-J. Stasia).

0005-2736/$ – see front matter © 2010 Elsevier B.V. All rights reserved.
doi:10.1016/j.bbamem.2010.08.002

response. Of all the family members in humans, Nox1, Nox3, and Nox4 are the most homologous to Nox2 [7–9].

In unstimulated phagocytes, the NADPH oxidase components are segregated into membrane and cytosolic locations. Upon activation, some cytosolic components ($p67^{phox}$, $p47^{phox}$, and $p40^{phox}$) become phosphorylated and migrate to the membrane-bound cyt b_{558} to form an active NADPH oxidase complex able to reduce molecular O_2 to $O_2^{\cdot-}$ [10–13]. Phosphorylation of NADPH oxidase subunits triggers establishment of a new network of protein–protein and protein–lipid interactions, resulting in activation of the oxidase. Activation requires phosphorylation events mainly on serine and threonine residues of $p47^{phox}$, $p67^{phox}$, $p40^{phox}$, $p22^{phox}$, and Nox2 via several kinases depending on the stimuli used [14–18]. In the case of $p47^{phox}$, it is well established that multiple phosphorylation events are required to relieve the self-inhibited structure and cause a conformational change in the protein, which leads to binding the membrane phosphoinositides and the proline-rich region (PRR) of $p22^{phox}$ with its PX and SH3 domains, respectively [19,20]. $p22^{phox}$ seems to be a docking site for $p47^{phox}$ [15,21–23]. Phosphorylated $p47^{phox}$ mediates $p67^{phox}$ and $p40^{phox}$ translocation to cyt b_{558}, with $p67^{phox}$ interacting simultaneously with $p47^{phox}$ and $p40^{phox}$ [24,25]. The $p67^{phox}$ subunit is also phosphorylated during the time course of NADPH oxidase assembly and activation, independently of $p47^{phox}$ [26]. In addition, there is some evidence for direct interaction between $p67^{phox}$ and cyt b_{558} during oxidase activation promoted by Rac-$p67^{phox}$ binding [27–33]. $p67^{phox}$ was shown to be involved in both assembly and activation of the oxidase complex, while $p47^{phox}$ proceeded as a positive effector and increased the affinity of $p67^{phox}$ with cyt b_{558} [34]. The role of $p40^{phox}$ and Rap1A is not clearly elucidated. PKCs play a dominant role, whatever the activation pathway involved, and are able to directly phosphorylate $p47^{phox}$ and/or $p67^{phox}$ [22,33,35]. Recently, it has been demonstrated that the potential cytosolic tail of Nox2 was phosphorylated during PMA activation by a PKC-dependent mechanism [18]. This is a new mechanism of NADPH oxidase activity's regulation by PKC phosphorylation events. MAPKs p38 and ERK1/2 are also involved in cytosolic factor phosphorylation, especially after G protein-coupled receptor-induced signal transduction (cytokines, fMLF) [14,36–38]. Specific synthesis of phosphoinositides is also a main regulatory mechanism in NADPH oxidase activation. Phosphoinositide-3-kinase (PI3K) plays a key role *via* synthesis of several intermediate phosphoinositides. Indeed, some protein kinases involved in phosphorylation of $p47^{phox}$ are directly or indirectly regulated by phosphoinositides [39,40]. Moreover, PI3K products, synthesized at the phagolysosomal membrane, can bind to $p47^{phox}$ and $p40^{phox}$ and thus take part in oxidase assembly and activation via the FcγR-dependent activation pathways [41]. Many agonists that stimulate superoxide anion production in phagocytes cause the release of arachidonic acid from membrane phospholipids by phospholipase A_2 (PLA_2) [42]. Recently, $cPLA_2$ has been described as a new partner for oxidase complex activation with direct binding to $p47^{phox}$ after the assembly of the NADPH oxidase complex [43].

Intracellular free calcium Ca^{2+} elevation is also a key regulating element in NADPH oxidase signaling pathways [44]. Indeed, activation of neutrophils by G protein-coupled receptors, such as fMLF, involves a rapid and transient elevation of cytosolic Ca^{2+} concentration, mainly from store-operated Ca^{2+} entry (SOCE). SOCE is a mechanism based on the depletion of endoplasmic reticulum (ER) Ca^{2+} stores, followed by extracellular Ca^{2+} entry through plasma membrane Ca^{2+} channels. This store depletion is mediated by the synthesis of inositol 1,4,5 triphosphate (InsP3), a Ca^{2+}-mobilizing second messenger, leading to the activation of channels located in the ER membranes: sarco(endo) plasmic reticulum Ca^{2+}-ATPase (SERCA) pumps. In addition, NADPH oxidase activation by fMLF requires a second Ca^{2+}-independent signal acting in synergy with Ca^{2+} influx from SOCE [45]. NADPH oxidase activation by Ca^{2+} influx during phagocytosis of opsonized particles is less well understood. According to Hallett's group, it requires Ca^{2+} signals divided in two temporally separated phases [46]. During NADPH oxidase activation, Ca^{2+} changes can regulate several potential targets in neutrophils. Ca^{2+} changes and phosphorylation are related events that are essential to the NADPH oxidase activation process. Conventional PKCs (a, βI, βII, and γ) require Ca^{2+} for cytosolic factor phosphorylation during NADPH oxidase activation by fMLF and opsonized particles [47]. In addition, some PLA_2 isoforms are activated by increased Ca^{2+} concentration and phosphorylation by MAPK [48]. Finally, phosphorylation probably influences not only the affinity of the subunits for each other, but also the stability of the NADPH oxidase complex [49]. Indeed, phosphorylation and hyperphosphorylation of NADPH oxidase components were proposed to trigger burst termination [50].

A recent study from our laboratory demonstrated the importance of the second intraplasmic D-loop of Nox2 (^{191}TSSTKTIRRS^{200}), i.e., three positively charged amino acids (Lys^{195}, Arg^{198} and Arg^{199}) in maintaining NADPH oxidase activity by controlling the electron transfer from FAD to O_2 in the transfected PLB-985 cells model [51]. In addition, replacing the D-loop of Nox2 by another D-loop of Nox1, Nox3, and Nox4 gave functional proteins. Moreover, the chimeric Nox2 protein containing the D-loop (^{191}TASTYAIRVS^{200}) of Nox4 (D-loop$_{Nox4}$-Nox2) supports superoxide overproduction compared to the wild type (WT) Nox2-transfected PLB-985 cells after PMA and fMLF stimulation. This suggests that the D-loop$_{Nox4}$ mutation optimizes NADPH oxidase activity. The aim of the present study was to characterize the superoxide overproduction in the D-loop$_{Nox4}$-Nox2 mutant upon stimulation of cells with different agonists and in a fully purified *in vitro* activation system. In addition, we have investigated whether the superoxide overproduction of this mutant was more effective against several microorganisms than the oxidase of the WT PLB-985 cells.

2. Materials and methods

2.1. Materials

Phorbol 12-myristate 13-acetate (PMA), dimethylformamide (DMF), diisopropylfluorophosphate (DFP), horseradish peroxidase (HRPO), formyl methionyl-leucyl-phenylalanine (fMLF), N-alpha-tosyl-L-lysyl-chloromethyl ketone (TLCK), zymosan, latex beads, ionomycin, diphenylene iodonium (DPI), luminol, and isoluminol were obtained from Sigma Chemical Co. (St Louis, MO, USA). Guanosine 5'-O-(3-thiotriphosphate) (GTPγS), NADPH, leupeptin, and pepstatin were from Roche (Meylan, France). Fetal bovine serum, RPMI 1640, Genistein, Alexa Fluor 633 goat-F(ab')$_2$ fragment anti-mouse IgG1 (H+L), dihydrorhodamine 123 (DHR) were from Invitrogen (Cergy Pontoise, France). Pseudomonas Isolation Agar (PIA) was from Difco, BD (Le Pont de Claix, France). Kinase inhibitors were from Calbiochem (Nottingham, UK). Monoclonal antibody specific for gp91phox 7D5 was purchased from MBL Medical and Biological Laboratories (Nakaku Nagoya, Japan).

2.2. Cell culture and granulocyte differentiation

WT, X-CGD PLB-985 cells and transfected X-CGD PLB-985 cells were maintained in RPMI-1640 containing 10% (v/v) heat-inactivated fetal bovine serum and 2 mM L-glutamine at 37 °C in a 5% CO_2 humidified atmosphere. After selection of transfected X-CGD PLB-985 cells, 0.5 mg/ml Geneticin was added to maintain the selection pressure. To induce granulocyte differentiation and expression of endogenous NADPH oxidase components, PLB-985 cells (2×10^5 cells/ml) were differentiated for 6 days with 0.5% (v/v) DMF. X-CGD PLB-985 cells correspond to *CYBB* knock-out PLB-985 cells as described by Dinauer's group [52]. WT Nox2 cells and D-loop$_{Nox4}$-Nox2 cells are X-CGD PLB-985 cells transfected with WT Nox2 cDNA and mutated Nox2

cDNA where the D-loop of Nox2 was replaced with the D-loop of Nox4 as previously described [51].

2.2.1. Human neutrophil isolation

Human neutrophils were purified from heparin blood samples of healthy donors after their informed consent, by sequential Ficoll-Hypaque differential density centrifugation as described elsewhere [53]. Neutrophils were resuspended in phosphate-buffered saline solution (PBS).

2.3. Cytosol and membrane fraction preparation from transfected PLB-985 cell lines

5.10^8 PLB-985 cells were treated with 3 mM DFP for 15 min on ice and resuspended in 1 ml PBS containing 1 mM phenylmethyl sulfonyl fluoride, 2 μM leupeptin, 2 μM pepstatin, and 10 μM TLCK. The cells were disrupted by sonication and the homogenate was centrifuged at 1000*g* for 15 min at 4 °C to remove unbroken cells and nuclei. The supernatant was withdrawn and centrifuged at 200,000*g* for 1 h at 4 °C. This high-speed supernatant was referred to as the cytosol and the pellet consisting of crude membranes was resuspended in the same buffer, as described before [51].

2.4. Purification and relipidation of cytochrome b_{558} from transfected PLB-985 cells

Cyt b_{558} was purified from transfected PLB-985 cells and relipidated accordingly, exactly as described [54]. In brief, purified cyt b_{558} was relipidated with 99% L-α-phosphatidylcholine (type XVI-E, Sigma-Aldrich) and 18:1 phosphatidic acid (DOPA). Cyt b_{558} purity was assessed using silver-stained SDS-PAGE and Western blotting. Cyt b_{558} was quantified by reduced-minus-oxidized difference spectroscopy using Soret band absorption at 426 nm. Liposomes were stored at −80 °C. The extinction molecular coefficient of oxidized cyt b_{558} at 414 nm ε is 131,000 M^{-1} cm^{-1}.

2.5. Purification of recombinant $p67^{phox}$, $p47^{phox}$, and Rac1

Full-length cDNAs encoding $p67^{phox,}$ $p47^{phox}$, and Rac1 were expressed in *Escherichia coli* as a glutathione S-transferase fusion protein using pGEX-2T. Protein expression was induced with isopropyl-1-thio-β-D-galactopyranoside (0.2 mM at 20 °C for $p67^{phox}$ and $p47^{phox}$, 0.1 mM at 37 °C for Rac1) for 3 h. Fusion proteins were purified by affinity on glutathione-Sepharose and were cleaved directly on the matrix using thrombin for $p47^{phox}$ and Rac1 [55,56]. $p67^{phox}$ was used without cleavage. The purity and cleavage of recombinant proteins were checked by SDS PAGE and Coomassie blue staining. The efficiency of enzymatic cleavage was more than 90% and the purity was over 95%. Recombinant proteins were stored at −20 °C until used.

2.6. Measurement of NADPH oxidase activity and Nox2 expression in intact cells

2.6.1. Simultaneous assessment of Nox2 protein expression and oxidase activity by flow cytometry

Differentiated transfected X-CGD PLB-985 cells (5×10^5) were resuspended in 100 μl of PBS containing 0.2% (p/v) bovine serum albumin and 1 mM $CaCl_2$. The cells were incubated with 5 μg/ml mAb 7D5 directed against an external epitope of Nox2 or irrelevant monoclonal IgG1 for 30 min on ice. The cells were washed twice and were incubated with Alexa Fluor 633 goat-F(ab')2 fragment anti-mouse IgG1 (H+L) for 30 min on ice. The cells were washed again in PBS supplemented with 0.9 mM $CaCl_2$ and 0.5 mM $MgCl_2$. Next, the cells were resuspended in 490 μl of PBS containing 0.9 mM $CaCl_2$ and 0.5 mM $MgCl_2$, 0.02% azide, and 20 mM glucose. Cells were incubated 10 min at 37 °C with 0.5 μM dihydrorhodamine (DHR) in the presence or absence of 5 μM DPI. Then the cells were activated with 80 ng/ml PMA 15 min at 37 °C. Finally, the cells were washed and kept on ice until flow cytometry analysis (FACScalibur, Becton Dickinson, Le Pont de Claix, France). Data were collected from 10,000 events and analysed using CellQuest software (BD PharMingen). All experiments were done in triplicate.

In some experiments Nox2 expression was evaluated by flow cytometry with the mAb 7D5 or irrelevant monoclonal IgG1, without (−) or with (+) permeabilization using 0.01% saponin (p/v) after fixation with 2% paraformaldehyde. The expression of cyt b_{558} was also examined by Western blot using mAb 48 and mAb 449 directed against Nox2 and $p22^{phox}$, respectively as previously described [51].

2.6.2. Measurement of H_2O_2 production by chemiluminescence

Differentiated PLB-985 cells or human neutrophils (5×10^5 cells/well in a 96-well plate) in PBS containing 0.9 mM $CaCl_2$, 0.5 mM $MgCl_2$, 20 mM glucose, 20 μM luminol, and 10 U/ml HRPO were stimulated with PMA (80 ng/ml), fMLF (4.10^{-7} M), ionomycin (2 μM), serum-opsonized zymosan OpZ (0.64 mg/ml) and Ig-opsonized latex beads ($3.5.10^8$ particles, 0.8 μm Ø). Relative light units (RLUs) were recorded at 37 °C over a time course of 15 min every 5 s or 60 min every 30 s in a luminoscan luminometer (Labsystems, Helsinki, Finland) connected to a computer. To determine the external H_2O_2 production, 20 μM luminol were replaced with 20 μM isoluminol (non-membrane-permeable) [57]. In some experiments, 5×10^5 cells were preincubated in PBS with kinase inhibitors Ro 31-8220 (1.25–20 μM) or wortmannin (6.25–100 nM) for 15 min, LY 294002 (6.25–100 μM), SB 203580 (5–20 μM), or genistein (25–200 μM) for 30 min at 37 °C before stimulation. Differentiated cells were also treated with PD 98059 (10–40 μM) overnight in a six-well plate in RPMI-1640 containing 10% (v/v) heat-inactivated fetal bovine serum and 2 mM L-glutamine at 37 °C in a 5% CO_2 humidified atmosphere. In other experiments, the cells were treated with GM-CSF (12 ng/ml) or TNFα (10 ng/ml) at 37 °C for 15 min in the chemiluminescence medium before activation with OpZ or fMLF [58].

2.7. NADPH oxidase activity in a cell-free system assay (CFS)

In vitro NADPH oxidase was measured using plasma membranes (30 μg and 100 μg) obtained from differentiated transfected PLB-985 cells and increasing amount of cytosol (50 to 300 μg) from human neutrophils, in a reaction mixture 20 μM GTPγS, 5 mM $MgCl_2$, and an optimal amount of arachidonic acid in a final volume of 100 μl. After incubation for 10 min at room temperature, oxidase activity was measured in the presence of 100 μM cytochrome *c* and 150 μM NADPH. The specificity of the $O_2^{\cdot-}$ production was checked by adding 50 μg/ml superoxide dismutase, which stopped the cytochrome *c* reduction [59]. Diaphorase activity was determined in the same conditions, except that cytochrome *c* was replaced with 50 μM iodonitrotetrazolium (INT) [60]. In some experiments, plasma membranes of PLB-985 cells and cytosol of neutrophils were replaced by purified cyt b_{558} (5 nM) and purified recombinant proteins $p67^{phox}$, $p47^{phox}$, and Rac1 preloaded with GTP-γ-S (1 μM). We added 10 μM FAD to the reaction medium when purified cyt b_{558} was used [31]. The oxidase activity was measured in presence of increasing amounts of arachidonic acid or of 10:0 phosphatidic acid [61].

2.8. Killing assay by human neutrophils and differentiated PLB-985 cells

Attenuated *Pseudomonas aeruginosa* strains (PAO-1) were selected from single colonies grown on Pseudomonas Isolation Agar (PIA) plates, transferred to Luria–Bertani (LB) broth medium and grown overnight at 37 °C [62]. Bacteria culture was restarted at 37 °C in LB broth until the exponential phase of bacterial growth followed on the basis of change in optical density (OD) at 600 nm. PAO-1 strains were

collected by centrifugation at 8500*g* for 5 min, washed twice in modified HEPES-buffered saline solution (15 mM HEPES, pH 7.4, 8 mM glucose, 4 mM KCl, 140 mM NaCl, 1 mM $MgCl_2$, 1 mM $CaCl_2$) and suspended at 5×10^7 or 5×10^8 PAO-1/ml; 2.5×10^6 cells were mixed with 2.5×10^6 or 2.5×10^7 colony forming units (CFUs) of PAO-1 (MOI, 1 or 10) in a final volume of 500 µl of modified HEPES-buffered saline solution supplemented with 10% (v/v) pooled human serum and shaken at 250 rpm at 37 °C. During incubation, 50-µl samples of the coincubation medium were collected, serially diluted in LB broth, and final samples were plated in duplicate on PIA plates. Colonies were counted after an overnight incubation at 37 °C. The microbicidal activity of cells against *Staphylococcus aureus* and *Candida albicans* was assessed according to a recently described method [63]. Briefly, neutrophils (4×10^6/ml) were incubated at 37 °C with serum-opsonized *S. aureus* (strain 502 A, ATCC 27217) and *C. albicans* from a clinical source at a microorganism/neutrophil ratio of 3:1 and 2:1, respectively, in HEPES-buffered saline solution containing 0.2% BSA and 1 mM each $CaCl_2$ and $MgCl_2$. Differentiated transfected PLB-985 cell microbicidal activity was evaluated in the same conditions but at a ratio of 1:2 for both. The transfected and CYBB-KO PLB-985 cells were cultured for at least 3 weeks and differentiated without antibiotics before their use for the killing assay. At indicated times of incubation, aliquots were diluted 50 times in water brought to pH 11.0 with NaOH 1 M. After 5 min at room temperature, samples were vortexed, diluted in 0.9% NaCl solution, and plated on Petri dishes. After overnight incubation, CFUs were counted and the percentage of killing was calculated with respect to the number of CFUs at time 0 of incubation.

2.9. Protein determination

Protein content was estimated using the Bradford assay [64] or the bicinchoninic acid method (Pierce®) [65].

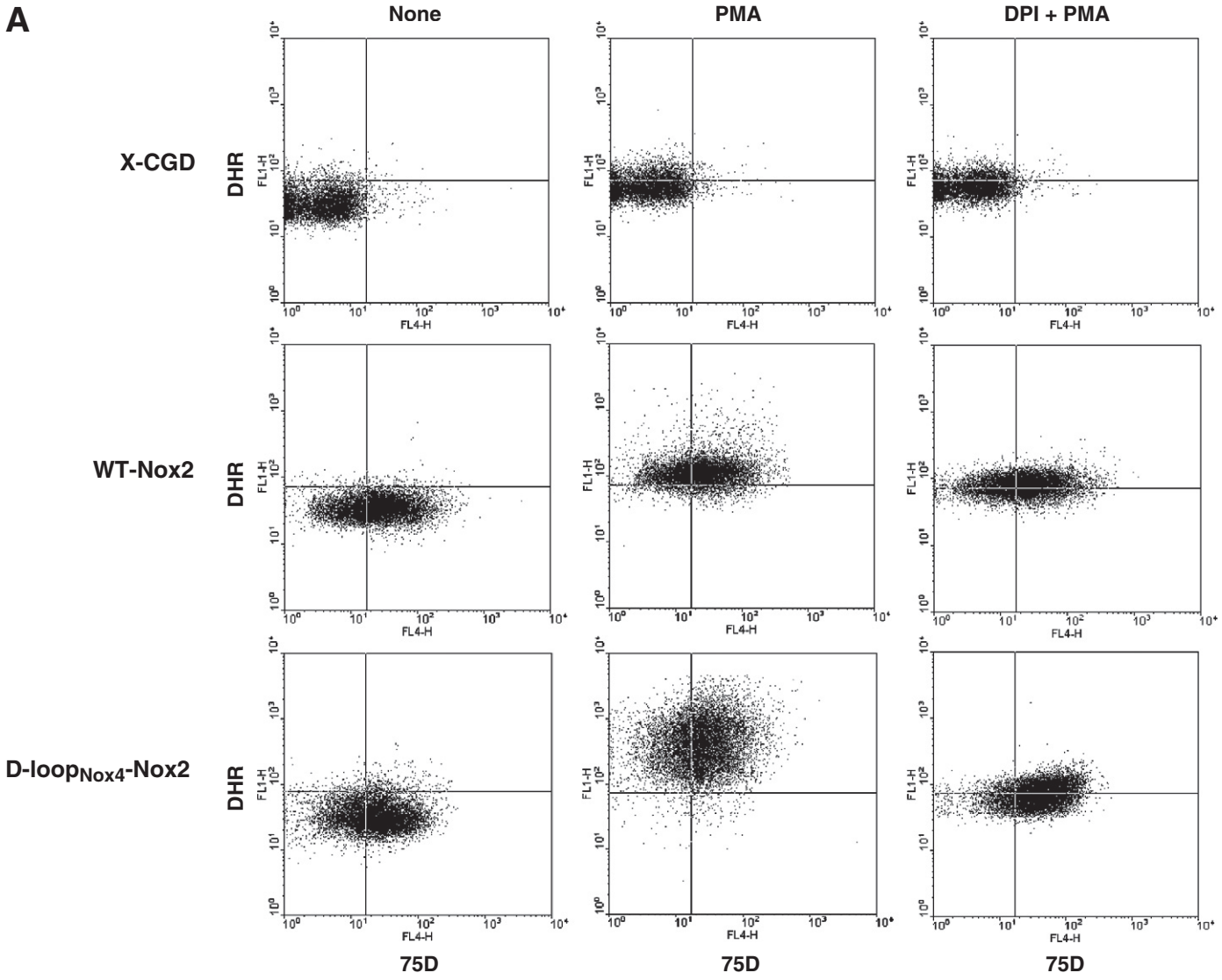

Fig. 1. Expression and NADPH oxidase activity of WT-Nox2 and D-loop$_{Nox4}$-Nox2 PLB-985 cells. (A) 5×10^5 differentiated transfected X-CGD PLB-985 cells were incubated with the Nox2 monoclonal antibody 7D5, combined with an Alexa Fluor 633 goat-anti-IgG (H+L), incubated with dihydrorhodamine 123 (DHR) and activated with 80 ng/ml PMA, as described in Materials and Methods. In some experiments, the NADPH oxidase activity was inhibited by 5 µM DPI. The fluorescence of the Alexa Fluor 633 goat-anti-IgG (H+L) and the H_2O_2 oxidized DHR was measured by flow cytometry. Results are from one experiment representative of three. (B) Western-blot analysis was performed with 1% Triton X100 soluble extract prepared from transfected WTNox2, DloopNox4-Nox2 and XCGD-PLB985 cells (50 µg of proteins each lane) as described in Materials and Methods. (C) Nox2 expression was evaluated by flow cytometry with the mAb 7D5 directed against an external epitope of Nox2 (white curves) or irrelevant monoclonal IgG1 (grey curves) without (−) or with (+) a permeabilization step using 0.01% saponin (p/v) after fixation with 2% paraformaldehyde.

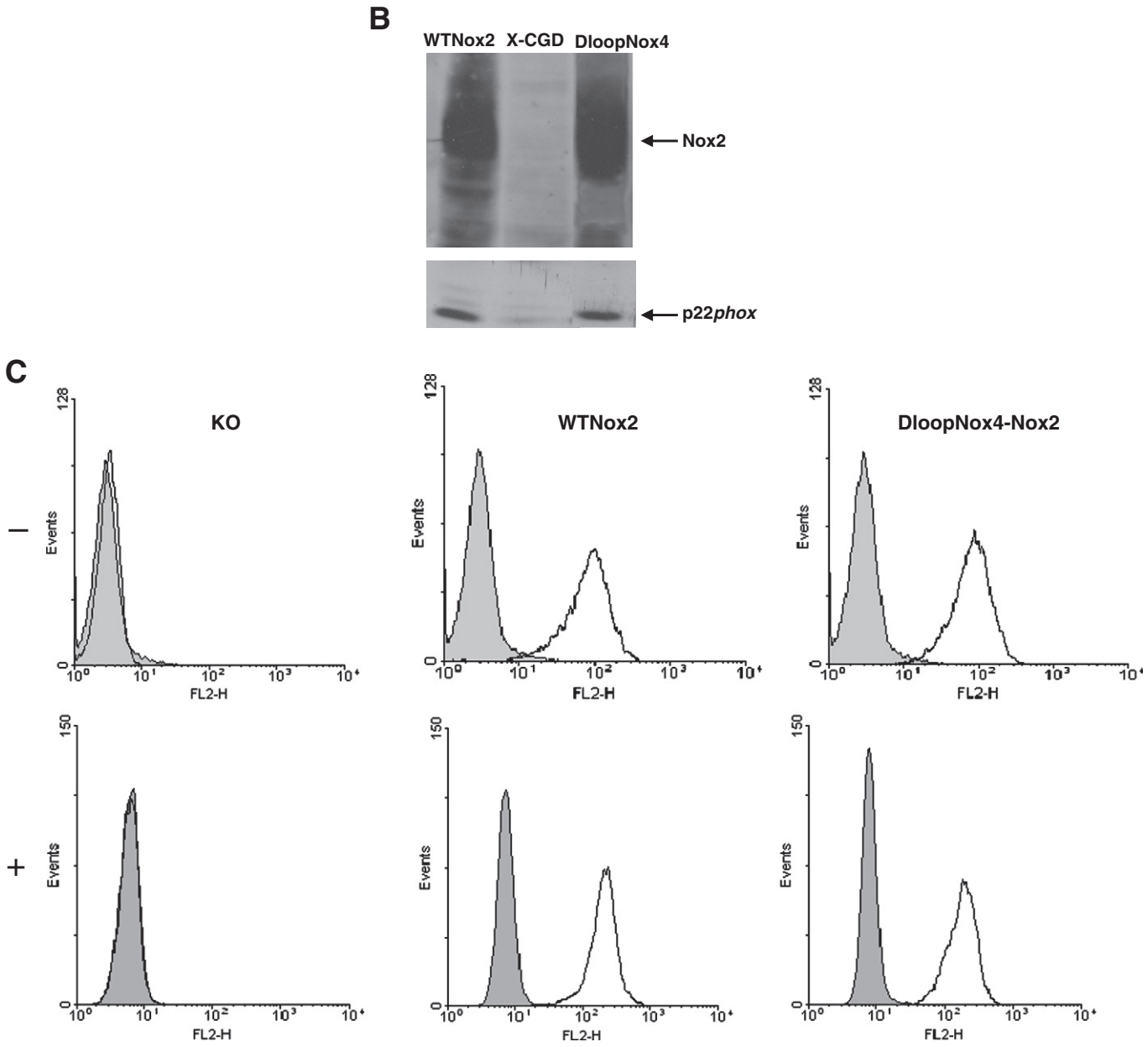

Fig. 1 (*continued*).

2.10. Statistics

All results are expressed as mean ± SD or SEM. Significant differences were identified using the Mann–Whitney test; $p<0.05$ was considered significant.

3. Results

3.1. Preferential superoxide overproduction of the D-loop$_{Nox4}$-Nox2 mutant cells with soluble versus particulate stimuli

We developed a useful method using FACS analysis to measure NADPH oxidase activity and Nox2 expression in transfected PLB-985 cells simultaneously, as described in Materials and Methods. NADPH oxidase activity was three to four times higher in the D-loop$_{Nox4}$-Nox2 mutant activated by PMA than in the WT-Nox2 transfected cells (Geometric (G) mean of 162.9 ± 37.9 and 491.9 ± 80.7, respectively), whereas Nox2 expression was equivalent in both cell types (G mean of 17.4 ± 4,0 and 22.1 ± 5.3, respectively) (Fig. 1A). NADPH oxidase was inhibited by 5 μM DPI, an inhibitor of cyt b_{558}. This control measurement was systematically performed every 3 months for defrosted clones of transfected PLB-985 cells. The same Nox2 expression was found in both cells types by western blotting (Fig. 1B). In addition the same intra and extracellular Nox2 expression in the WT-Nox2 and D-loop$_{Nox4}$-Nox2 cells was found by flow cytometry analysis with or without permeabilization by 0.01% saponin (p/v) (Fig. 1C).

H_2O_2 production in intact differentiated D-loop$_{Nox4}$-Nox2 mutant cells was measured using luminol-amplified chemiluminescence after soluble and particulate stimuli activation (Fig. 2; Table 1). All the experiments were done in triplicate and reproduced at least four times with each stimulus ($n=4$–12). H_2O_2 overproduction was always observed in the D-loop$_{Nox4}$-Nox2 cells activated by soluble (PMA, fMLF, and ionomycin) and particulate [IgG-opsonized latex beads (IgG-LB), serum-opsonized zymosan (OpZ)] stimuli compared to the WT-Nox2-transfected cells (Fig. 2). However, although the

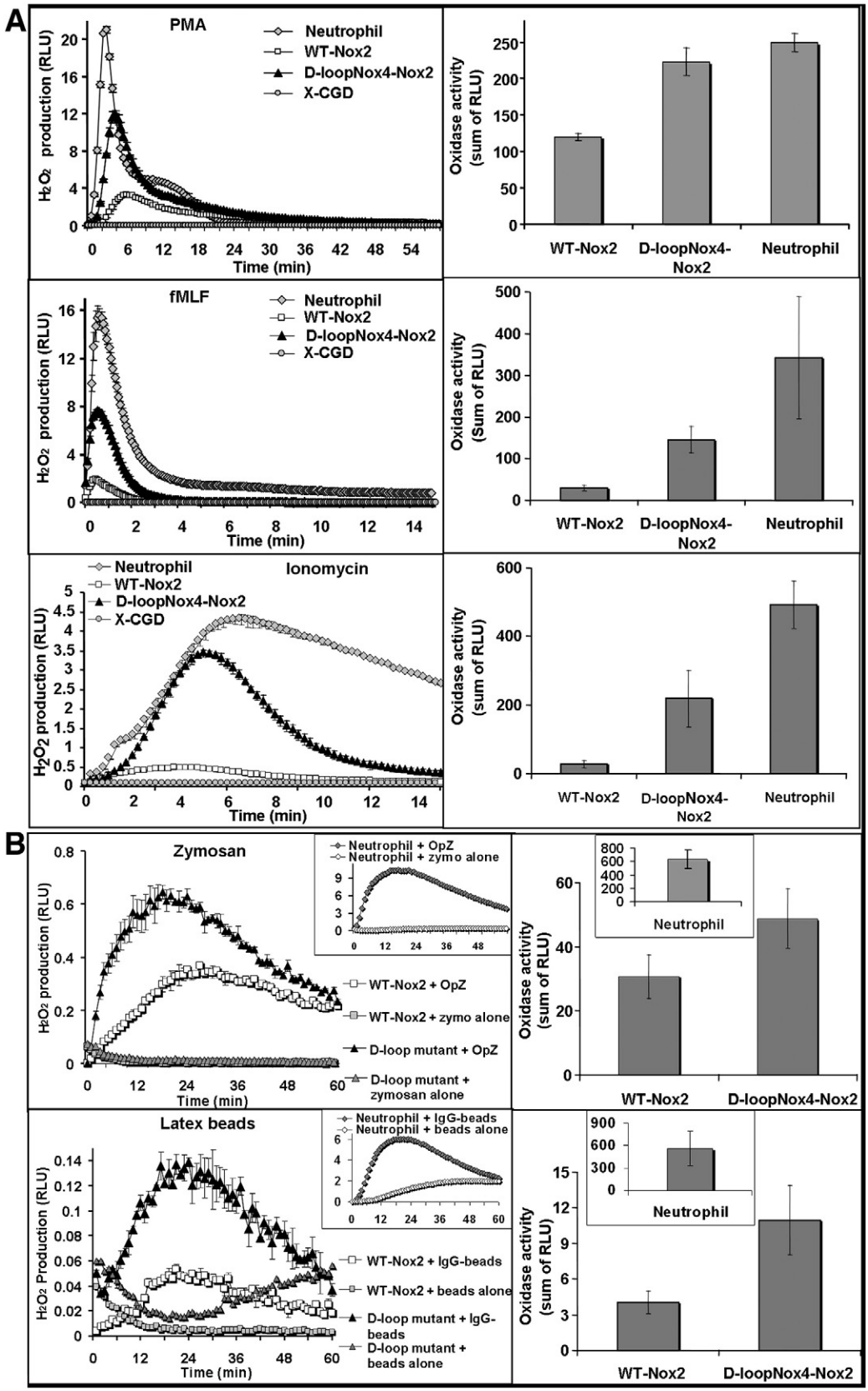

Fig. 2. NADPH oxidase activity in intact PLB-985 cells and human neutrophils induced by various soluble or particulate agonists. (A) Kinetics and total H_2O_2 production measured by luminol-amplified chemiluminescence from 5×10^5 differentiated transfected X-CGD PLB-985 cells and human neutrophils after activation with soluble agonists PMA for 60 min, and fMLF or ionomycin for 15 min (B) after activation with particulate agonists OpZ (0.64 mg/ml) and IgG-opsonized latex beads ($3.5.10^8$ particles) as described in Materials and Methods. Kinetics presented are mean ± SD of a triplicate from one experiment representative of at least four independent determinations. Total H_2O_2 production results represent the mean ± SD of H_2O_2 production of independent experiments ($n=4$–12).

Table 1
NADPH oxidase activity in transfected PLB-985 cells and human neutrophils induced by various agonists. H_2O_2 production was measured by luminol-amplified chemiluminescence from 5×10^5 differentiated transfected PLB-985 cells and neutrophils for 60 min after PMA, OpZ, IgG-opsonized latex beads activation, and for 15 min after fMLF or ionomycin stimulation. Values represent the mean ± SD of at least four independent determinations ($n=4$–12). Total H_2O_2 production represents the sum of RLU measured over 15 or 60 min. In the last column, this production is expressed as the percentage of the value obtained with WT-Nox2 cells. "Peak-RLUmax" indicates the maximal value obtained and Tmax the time to reach the "peak-RLUmax." The duration is the time between stimulation and a decrease to 10% of the peak value. With particulate agonists, the time results are expressed as a percentage of the peak value at 60 min. NR: not relevant. D-loop$_{Nox4}$-Nox2 cells compared with WT-Nox2 cells: *$p<0.05$. Items under brackets represent the times of the NADPH oxidase increase in each cell types against the oxidase activity of the WT-Nox2 cells.

Soluble stimuli		Total H_2O_2 production (RLU)		Tmax (min)	Peak-RLUmax (RLU)		Duration (min)	% of WT-Nox2 H_2O_2 production
PMA	X-CGD	0.46 ± 0.14		NR	NR		NR	0
	WT-Nox2	119.57 ± 4.94		6.45 ± 0.72	2.61 ± 0.44		58.1 ± 3.9	100
	D-loopNox4-Nox2	223.03 ± 18.58 *	(2×)	4.36 ± 0.56 *	10.13 ± 1.84 *	(×4)	30.4 ± 4.0*	187
	Neutrophil	249.22 ± 12.57*	(2×)	3.38 ± 0.22*	17.64 ± 2.81*	(×7)	20.9 ± 1.4*	208
fMLF	X-CGD	0.35 ± 0,03		NR	NR		NR	1
	WT-Nox2	29.69 ± 6.64		0.65 ± 0.16	1.59 ± 0.48		2.8 ± 0.3	100
	D-loopNox4-Nox2	145.95 ± 32.64*	(×5)	0.67 ± 0.15	8.28 ± 1.51*	(×5)	2.8 ± 0.3	492
	Neutrophil	341.92 ± 146.35	(×11)	0.64 ± 0.04	14.72 ± 6.81	(×10)	4.7 ± 1.4	1,152
Lonomycin	X-CGD	0.37 ± 0.19		NR	NR		NR	1
	WT-Nox2	27.55 ± 11.02		4.22 ± 1.07	0.39 ± 0.19		12.8 ± 1.7	100
	D-loopNox4-Nox2	218.71 ± 81.98 *	(×8)	5.25 ± 0.93	3.03 ± 1.34 *	(×8)	14.1 ± 1.1	794
	Neutrophil	492.96 ± 69.21	(×18)	6.61 ± 0.48	4.04 ± 0.40	(×10)	>15	1,789
Particulate stimuli		**Total H_2O_2 production (RLU)**		**Tmax (min)**	**Peak-RLUmax (RLU)**		**% peak value at 60 min**	**% of WT-Nox2 H_2O_2 production**
Serum-OpZ	X-CGD	0.33 ± 0.14		NR	NR		NR	1
	WT-Nox2	30.72 ± 6.78		20.81 ± 3.27	0.40 ± 0.09		38.4 ± 4.2	100
	D-loopNox4-Nox2	48.84 ± 9.30*	(×1,5)	20.00 ± 3.99	0.60 ± 0.13	(×1,5)	36.1 ± 8.6	159
	Neutrophil	629.76 ± 140.74	(×20)	16.50 ± 3.08	8.39 ± 1.81	(×21)	25.4 ± 11.4	2,050
IgG-opsonized beads	X-CGD	0.43 ± 0.24		NR	NR		NR	10
	WT-Nox2	4.04 ± 0.95		18.75 ± 3.42	0.06 ± 0.02		26.9 ± 5.2	100
	D-loopNox4-Nox2	10.90 ± 3.05*	(×3)	22.90 ± 1.16	0.13 ± 0.04 *	(×2)	42.3 ± 1.8 *	270
	Neutrophil	557.72 ± 231.92	(×138)	18.90 ± 5.48	6.79 ± 2.44*	(×113)	41.8 ± 13.8 *	13,805

oxidase activity of the D-loop$_{Nox4}$-Nox2 cells stimulated with soluble stimuli was of the same order to what we observed in human neutrophils (Fig. 2A), the oxidase activity of this mutant measured after particulate stimuli was approximately 20–60 times lower than neutrophil oxidase activity (Table 1). In addition, H_2O_2 production was highly dependent on serum or IgG opsonization. The Peak-Tmax and the duration values for the PMA and fMLF activation of the D-loop$_{Nox4}$-Nox2 mutant were also similar to the respiratory burst kinetics of the human neutrophils. This was not the case, however, for the WT Nox2-transfected PLB-985 cells (Table 1). The highest superoxide-generating activity obtained with the D-loop$_{Nox4}$-Nox2 mutant was observed after fMLF and ionomycin stimulation. Indeed, total H_2O_2 production and Peak-RLUmax of the D-loop$_{Nox4}$-Nox2 mutant were five and eight times higher, respectively, than for the WT-Nox2 cells when stimulated with fMLF and ionomycin, respectively and different activation kinetics, especially a shorter duration of the burst compared to neutrophils (Fig. 2). In conclusion, H_2O_2 overproduction of the D-loop$_{Nox4}$-Nox2 mutant was evident with soluble activators, particularly with ionomycin, where the Peak-RLUmax was nearly comparable to that of human neutrophils. Nevertheless, particulate stimuli and particularly IgG-LB, failed to reasonably activate the NADPH oxidase in PLB-985 cells compared to human neutrophils even if the H_2O_2 production of the D-loop$_{Nox4}$-Nox2 mutant was even higher than WT-Nox2-transfected cell H_2O_2 production.

3.2. NADPH oxidase activity in a reconstituted cell-free system

We then evaluated the potential ability of the mutated D-loop$_{Nox4}$-Nox2 cyt b_{558} of plasma membranes to overproduce superoxide anions in a cell-free system (CFS) assay in the presence of NADPH, GTPγS, increasing amounts of human neutrophil cytosol, and an adequate concentration of arachidonic acid (AA) (Fig. 3A). The NADPH oxidase activity was identical in the membranes of the mutant D-loop$_{Nox4}$-Nox2 as in the WT-Nox2 PLB-985 cells for all the cytosol concentrations used (range, 0–300 μg). The same result was obtained for diaphorase activity, which reflects the electron transfer from NADPH to FAD (Fig. 3A). We tried to evaluate the reconstituted oxidase activity with phosphatidic acid but some problems of solubility were encountered with high concentration of membranes. This was not found in the simplified CFS using purified cyt b_{558}. Cyt b_{558} was purified from 10^{10} WT-Nox2 or D-loop$_{Nox4}$-Nox2 PLB-985 cells with single-step immunoaffinity chromatography, as previously described [54]. WT and mutated cyt b_{558} were purified with a yield of 6–9%, a purification factor of 180 with a specific activity of about 12,000 pmol/mg protein. The turnover of WT and mutated purified cyt b_{558} was measured in a CFS assay with optimal conditions in the presence of saturating amounts of recombinant proteins p67^{phox}, p47^{phox}, and Rac1 as described in Materials and Methods. When purified and relipidated cyt b_{558} was used, the oxidase activity was significantly higher for D-loopNox4-Nox2 than for WT Nox2 ($p=0.04$, $n=5$), only when PA was used as activating agent. In contrast no significant difference was found with arachidonic acid (Fig. 3B) In conclusion, PA mimics the activation process of the superoxide overproduction of the D-loop-Nox2 mutant observed in intact cells better than AA.

3.3. Effect of the cytosolic calcium increase on the NADPH oxidase activity of D-loop$_{Nox4}$-Nox2 PLB-985 cells

As demonstrated above, ionomycin, a potent calcium ionophore, was able to trigger the best superoxide overproduction in the D-loop$_{Nox4}$-Nox2 cells compared to the WT-Nox2 cells (Fig. 2A). In addition, intracellular Ca^{2+} is involved in the signaling pathway during NADPH oxidase activation after fMLF stimulation, which also produces a notable ROS overproduction in the D-loop$_{Nox4}$-Nox2 cells. Then we studied the influence of Ca^{2+} variation on the oxidase activity of the D-loop$_{Nox4}$-Nox2 cells. We found that an extracellular

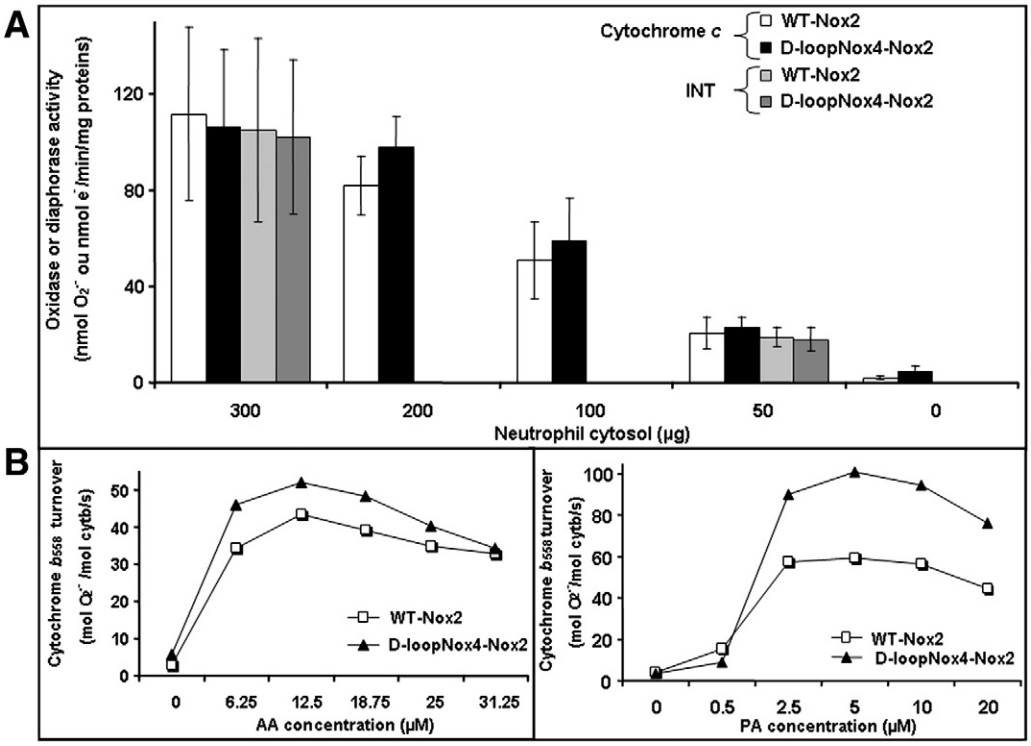

Fig. 3. NADPH oxidase and diaphorase activity of transfected X-CGD PLB-985 cells in a cell-free system. (A) NADPH oxidase and diaphorase activity were reconstituted in a cell-free-system (CFS) with purified plasma membranes from transfected X-CGD PLB-985 cells in the presence of decreasing amounts of neutrophil cytosol and activated with GTPγS and arachidonic acid as described in Materials and Methods. Oxidase activity was measured in the presence of 100 µM cytochrome c and diaphorase activity in the presence of 50 µM iodonitrotetrazolium (INT). Data are presented as mean ± SD and representative of three independent experiments ($n = 3–7$). (B) NADPH oxidase activity was reconstituted in a CFS using purified and relipidated cyt b_{558} (5 nM) from differentiated transfected X-CGD PLB-985 cells as described in [54] and recombinant cytosolic proteins $p47^{phox}$, $p67^{phox}$, and Rac1 (1 µM) activated by increasing amounts of AA or PA. Results are representative of one experiment in three.

deprivation of calcium, achieved by increasing extracellular EGTA, decreased oxidase activity in both $loop_{Nox4}$-Nox2 and WT-Nox2 cells. However, the oxidase activity of the D-$loop_{Nox4}$-Nox2 mutant was less affected by EGTA than the WT-Nox2 cells, especially at the 0.5-mM concentration (Fig. 4A). This result was confirmed by experiments done with BTP2, an inhibitor of SOCE that blocks calcium influx.

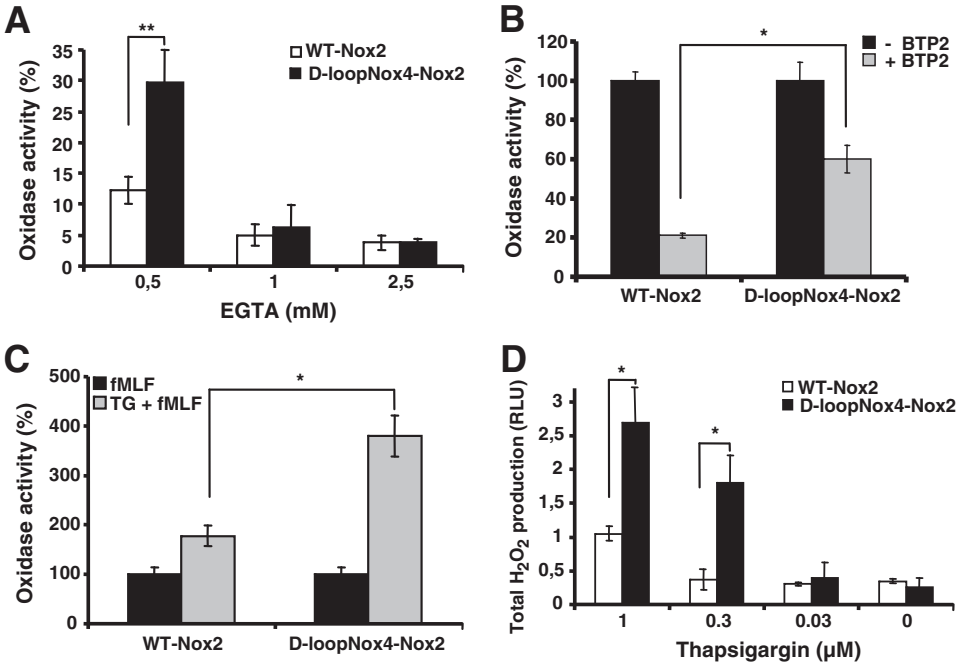

Fig. 4. Role of Ca^{2+} influx on NADPH oxidase activity of differentiated transfected X-CGD PLB-985 cells stimulated by fMLF. Differentiated PLB-985 cells (5×10^5 cells) were incubated in PBS at 37 °C with increasing amounts of EGTA (A) or 10 µM BTP2 for 5 min (B), or 1 µM thapsigargin (C) and then activated with fMLF (4×10^{-7} M). Cells were also activated by increasing amounts of thapsigargin alone (D). H_2O_2 production was measured by luminol-amplified chemiluminescence as described in Materials and Methods. Results in (A), (B), and (C) are expressed in percentages by dividing the total RLU value obtained for each type of cell in the presence of inhibitors/activators by the value obtained without them and represent the mean ± SD of three to six independent experiments. Results presented in (D) are the mean ± SD of total H_2O_2 production of four to five experiments—D-$loop_{Nox4}$-Nox2 cells compared with WT-Nox2 cells: $^*p<0.05$, $^{**}p<0.01$.

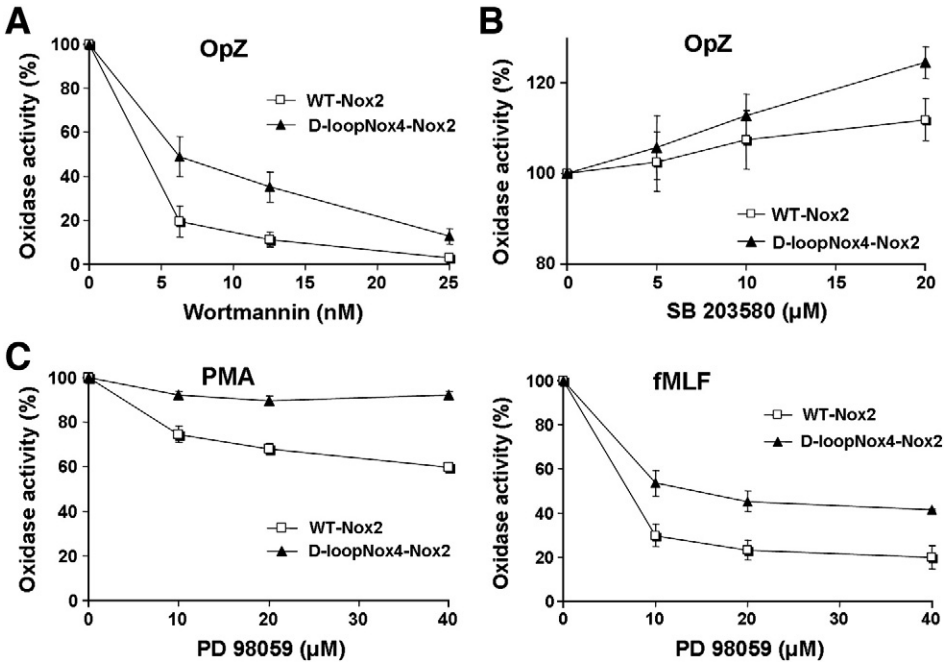

Fig. 5. Effect of phosphorylation events on NADPH oxidase activity of differentiated transfected X-CGD PLB-985 cells—Kinetics of H_2O_2 production was measured by luminol-amplified chemiluminescence from 5×10^5 transfected PLB-985 cells preincubated with increasing amounts of Wortmannin (A), SB 203580 (B), or PD 98059 (C), and activated with fMLF (4×10^{-7} M), PMA (80 ng/ml) or OpZ (0.64 mg/ml) as described in Materials and Methods. Results are expressed in percentages by dividing the total RLU value obtained for each type of cell in the presence of inhibitors by the value obtained without inhibitors and represent the mean ± SD of three to five independent experiments.

Indeed, in the presence of 10 μM BTP2 the oxidase inhibition of the D-loop$_{Nox4}$-Nox2 cells was 40% versus 80% for the WT-Nox2 cells (Fig. 5B). The intracellular Ca^{2+} store depletion that secondarily activates Ca^{2+} influx through SOCE is obtained by thapsigargin (TG) treatment. We found that the oxidase activity was approximately 2.5–4 times higher in the D-loop$_{Nox4}$-Nox2 cells than in the WT-Nox2 cells after stimulation by 1 or 0.3 μM TG, respectively (Fig. 5D). After fMLF activation of pretreated PLB-985 cells with 1 μM thapsigargin, D-loop$_{Nox4}$-Nox2 cells still showed a superoxide overproduction (Fig. 5C). In conclusion, the superoxide overproduction of the D-loop$_{Nox4}$-Nox2 cells after fMLF and ionomycin activation can be explained in part, by a change in Ca^{2+} sensitivity.

3.4. Influence of phosphorylation events on the NADPH oxidase activity of the D-loop$_{Nox4}$-Nox2 PLB-985 cells

We demonstrated above that the superoxide overproduction of the D loop$_{Nox4}$-Nox2 mutant was related to a change in Ca^{2+} increase

Table 2
Effect of kinase inhibitors on fMLF, PMA and OpZ induced ROS production in differentiated transfected PLB-985 cells. 5×10^5 PLB-985 cells were incubated in PBS at 37 °C with Ro31-8220 or Wortmannin for 15 min, SB 203580 for 30 min, or PD 98059 overnight, then activated with fMLF (4×10^7 M), PMA (80 ng/ml) and OpZ (0.64 mg/ml). Values are expressed as a percentage of inhibition of control production without inhibitors. Data are presented as mean ± SD and representative of at least three independent determinations ($n=3$–5). D-loop$_{Nox4}$-Nox2 cells compared with WT-Nox2 cells: *$p<0.05$.

	Ro 31-8220			Wortmannin		
	Concentration (μM)	WT-Nox2	D-loop$_{Nox4}$-Nox2	Concentration (nM)	WT-Nox2	D-loop$_{Nox4}$-Nox2
OpZ	5	1.6 ± 5.5	4.4 ± 7.6	6.25	80.4 ± 7.1	50.9 ± 9.1*
	10	26.1 ± 8.1	29.0 ± 6.5	12.5	88.9 ± 3.3	64.9 ± 6.7*
	20	94.3 ± 0.4	89.8 ± 0.8	25	96.9 ± 0.9	87.2 ± 3.6*
PMA	1.25	39.5 ± 4.3	35.0 ± 1.8	25	5.0 ± 3.7	−5.1 ± 1.5
	2.5	78.0 ± 3.2	82.0 ± 4.1	50	3.5 ± 1.6	−3.4 ± 1.7
	5	99.6 ± 0.1	99.3 ± 0.3	100	3.9 ± 1.3	−5.8 ± 2.4
fMLF	1.25	20.3 ± 7.1	7.6 ± 7.2	25	47.0 ± 6.6	45.5 ± 5.3
	2.5	35.7 ± 11.6	28.9 ± 13.0	50	53.6 ± 4.7	52.7 ± 4.1
	5	95.0 ± 2.9	88.1 ± 5.1	100	63.8 ± 4.6	63.9 ± 3.2
	PD 98059			SB 203580		
	Concentration (μM)	WT-Nox2	D-loop$_{Nox4}$-Nox2	Concentration (μM)	WT-Nox2	D-loop$_{Nox4}$-Nox2
OpZ	10	24.7 ± 6.3	19.3 ± 2.6	5	−2.6 ± 6.6	−5.7 ± 7.1
	20	32.2 ± 7.7	24.6 ± 3.8	10	−7.4 ± 6.5	−12.9 ± 4.7
	40	39.6 ± 4.1	30.5 ± 2.7	20	−12.0 ± 4.8*	−24.6 ± 3.5*
PMA	10	25.3 ± 3.6	7.8 ± 1.8*	5	4.2 ± 5.4	0.6 ± 2.4
	20	32.2 ± 2.5	10.2 ± 2.1*	10	6.9 ± 3.2	4.0 ± 2.5
	40	40.3 ± 2.2	7.9 ± 1.9*	20	8.5 ± 1.2	5.3 ± 1.2
fMLF	10	70.2 ± 5.0	46.5 ± 6.0*	5	38.2 ± 6.4	55.4 ± 3.7
	20	76.8 ± 4.4	54.7 ± 4.8*	10	53.6 ± 4.9	62.9 ± 2.9
	40	79.9 ± 5.3	58.6 ± 0.5*	20	63.7 ± 2.5	71.2 ± 5.8

sensitivity. As the majority of phosphorylation events occurring during fMLF or ionomycin or OpZ-dependent NADPH oxidase activation require an increase of intracellular Ca^{2+}, we examined the involvement of the phosphorylation events on superoxide overproduction by the D-loop$_{Nox4}$-Nox2 mutant. We used increasing amounts of specific kinase inhibitors in a chemiluminescence assay as described in Materials and Methods. A similar inhibitory effect of Ro31-8220, which substantially inhibits the two conventional isoforms PKCα and PKCβ, was shown in both D-loop$_{Nox4}$-Nox2 cells and WT-Nox2 cells after PMA, fMLF, and OpZ activation (Table 2). Then the implication of the PI3K pathway was tested using Wortmannin or LY-294002. Even with high concentrations of both, no inhibition of oxidase activity was observed in either cell type after PMA activation. With fMLF, the inhibition was partial and equivalent in both cell types (Table 2). The most interesting result regarding the effect of these inhibitors was observed after OpZ activation. With the smallest concentrations of both drugs, a drastic inhibitory effect was detected on oxidase activity of the WT-Nox2 cells (50–80% inhibition, Wortmannin-LY-294002), whereas in the D-loop$_{Nox4}$-Nox2 cells the inhibition was less pronounced (25–50%) (Fig. 5A). This difference was still observed with increasing amounts of PI3K inhibitors. Then PLB-985 cells were incubated overnight with 10, 20, or 40 μM PD98059, an ERK1/2MAPK inhibitor. The first striking observation was that no inhibitory effect of PD98059 on oxidase activity was observed in the D-loop$_{Nox4}$-Nox2 cells stimulated with PMA, whereas 40% inhibition was obtained in the WT-Nox2 cells with a maximal PD98059 concentration (40 μM) (Fig. 5C). Similarly, after fMLF stimulation, PD98059 was more efficient in inhibiting the oxidase activity of the WT Nox2 cells, than that of the D-loop$_{Nox4}$-Nox2 cells (Fig. 5C). However, a slight but similar inhibitory effect of PD98059 was seen in both cell types activated by OpZ (Table 2). The same inhibitory effect was obtained using U0126, another ERK1/2MAPK inhibitor (data not shown). Finally, we used SB203580, which prevents p38 MAPK activation, to compare the role of this kinase pathway on the D-loop$_{Nox4}$-Nox2 and the WT-Nox2 oxidase activation. According to our results, p38MAPK was not involved in PMA-induced oxidase activity of the D-loop$_{Nox4}$-Nox2 and the WT-Nox2 cells, although it occupies an important place in fMLF-induced oxidase activity, but its effect was comparable in both cell types (Table 2). Surprisingly, p38 MAPK inhibition triggered an enhancement of total H_2O_2 production in PLB-985 cells stimulated with OpZ and more pronounced in the D-loop$_{Nox4}$-Nox2 cells (Fig. 5B).

3.5. Killing power of the D-loop$_{Nox4}$-Nox2 PLB-985 cells against microorganisms

To determine whether ROS overproduction of the D-loop$_{Nox4}$-Nox2 PLB-985 cells improves their microbicidal power, the killing activity against microorganisms was evaluated. We took care to cultivate the transfected and KO PLB-985 cells without antibiotics during at least 3 weeks before the killing experiments. The killing activity of the D-loop$_{Nox4}$-Nox2, WT-Nox2, X-CGD PLB-985 cells, and human neutrophils against an attenuated strain of *P. aeruginosa* PAO-1 was measured for 60 min with an MOI of 1 and 10 for PLB-985 cells and neutrophils, respectively (Fig. 6). As expected, the bactericidal power of the PLB cells was clearly below that of the neutrophils. However, the killing activity of the D-loop$_{Nox4}$-Nox2 PLB-985 cells, over 15–60 min of incubation, was always significantly higher than that of the WT-Nox2 PLB cells. In addition we controlled that the bactericidal power of the WT-Nox2 PLB-985 cells was comparable to that of the original WT PLB-985 cells (data not shown). X-CGD PLB-985 cells, in spite of a lack of Nox2 protein, were able to kill *P. aeruginosa* at 45 min and 60 min of contact, suggesting a NADPH oxidase-independent killing mechanism against this bacterium. Nevertheless, the killing activity of X-CGD PLB-985 cells was always lower than that observed in the WT-Nox2 and the D-loop$_{Nox4}$-Nox2 PLB-985 cells. Regarding *S. aureus* and *C. albicans* killing, the ROS production of the PLB-985 cells (mutant or WT) was not sufficient to eliminate them efficiently after 10 min of incubation (data not shown).

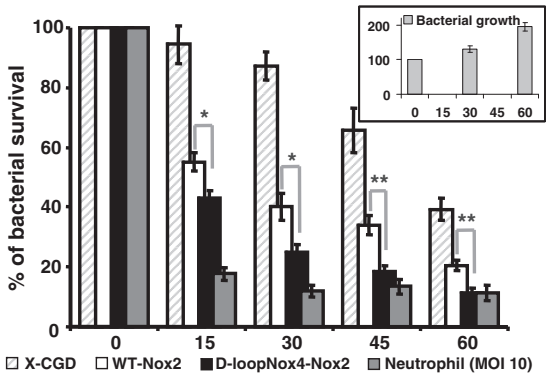

Fig. 6. Killing activity of differentiated transfected X-CGD PLB-985 cells and human neutrophils against *P. aeruginosa*. The killing of *P. aeruginosa* PAO-1 was evaluated by following the decrease of survival colony number after co-incubation with cells for 0 to 60 min at MOI 1 (PLB-985 cells) or MOI 10 (neutrophils), as described in Materials and Methods. Mean ± SEM of at least five independent experiments are presented ($n = 5$–9). D-loop$_{Nox4}$-Nox2 cells compared with WT-Nox2 cells at each incubation time: $^{*}p<0.05$; $^{**}p<0.01$. Insert in the figure represents the growth of microorganisms in absence of PLB-985 cells.

4. Discussion

The NADPH oxidase of professional phagocytes is a crucial component of the innate immune response due to its fundamental role on reactive oxygen species production as powerful microbicidal agents. Nox2 is the essential catalytic element for electron transfer from NADPH to FAD and to finally reduce molecular oxygen, after optimal association of cytosolic factors with cyt b_{558} in the plasma membrane. We previously demonstrated that the second intraplasmic D-loop ^{191}TSSTKTIRRS^{200} of Nox2, i.e., charged amino acids, were essential for electron transfer from FAD to oxygen. Moreover, replacement of the D-loop of Nox2 with the D-loop of its homolog of nonphagocytic oxidase Nox4 overproduced ROS compared to WT PLB-985 cells after PMA and fMLF stimulation. This was the first description of mutations leading to an abnormal increase of oxidase activity [51].

In this work we show a superoxide overproduction of the D-loop$_{Nox4}$-Nox2 PLB-985 cells with particulate stimuli (OpZ and IgG-LB). However the oxidase activity was particularly low with IgG opsonized latex beads in wild type and mutant PLB-985 cells (about 60 times less than that in human neutrophils). A low NADPH oxidase activity after Fcγ-stimulated activation by IgG-latex in PLB-985 cells was also recently reported [41]. Several explanations can be given, the first one being that DMF-differentiated PLB-985 cells show a defect in the phagocytic process of IgG opsonized particles. This can be ruled out because we and others have shown perfect phagocytosis of IgG-LB or OpZ by PLB-985 cells using confocal microscopy [31,51,66]. The more probable explanation is that one or several molecules of the IgG-LB signaling pathway are missing leading to partial activation of the NADPH oxidase complex in differentiated PLB-985 cells. A striking point was that the H_2O_2 overproduction in the D-loop$_{Nox4}$-Nox2 PLB-985 cells is preferentially obtained after soluble stimuli activation (X5-8) compared to particulate stimuli (X2). The absence of specific granules containing cyt b_{558} could explain the low NADPH oxidase activity seen in PLB-985 cells specially when activated by particulate stimuli where the intraphagosomal NADPH oxidase activity must be supplied longer than in the case of soluble stimuli [50]. The presence of specific granules in differentiated PLB-985 cells is controversial [67,68]. In our hands we did not find lactoferrin and gelatinase

(markers of specific granules) after differentiation of PLB-985 cells in presence of Nudridoma SP (manuscript in preparation). In addition a recent paper shows that specific granules were present only after dibutiryl AMPc differentiation [69]. In a previous work we also found that PLB-985 cells contained seven to ten times less cyt b_{558} than human neutrophils [31]. This may be due to the lack of specific granules containing cyt b_{558} in DMF-differentiated PLB-985.

Maximal superoxide overproduction was obtained with soluble stimuli and more specifically with ionomycin and fMLF in D-loop$_{Nox4}$-Nox2 PLB-985 cells. As we know both stimuli activate the NADPH oxidase by Ca^{2+}-dependent signaling pathways. Superoxide overproduction was probably related to Ca^{2+}-dependent mechanisms. Indeed, superoxide overproduction was detected after thapsigargin treatment, which induces intracellular Ca^{2+} store depletion and secondarily activates Ca^{2+} influx through SOCE, as if the D-loop$_{Nox4}$-Nox2 mutant was more sensitive to an intracellular Ca^{2+} increase than the WT-Nox2 cells. In contrast, external deprivation of Ca^{2+}, using a moderate amount of EGTA or blockage of the SOCE by BTP2, which inhibits calcium influx, has a less inhibitory effect on the oxidase activity of the mutant compared to the WT-Nox2 cells. Probably the high sensitivity of the D-loop$_{Nox4}$-Nox2 mutant to Ca^{2+} to trigger the oxidase activation lowers the amount of Ca^{2+} needed. It can be hypothesized that the conformation of the D-loop$_{Nox4}$-Nox2 mutant favors the assembly process even in presence of calcium traces.

Although an intracellular calcium increase is not sufficient to reach full activation of the NADPH oxidase complex (as demonstrated by the low oxidase activation level with thapsigargin alone), a second signal in combination with Ca^{2+} influx is most of the time necessary to fully activate the NADPH oxidase complex [45]. The main additional event related to intracellular Ca^{2+} increase required to activate the NADPH oxidase complex is phosphorylation [44], which can be Ca^{2+}-dependent and takes place mainly on cytosolic factors p47^{phox}, p67^{phox}, and p40^{phox} via kinases such as PKCs, p38MAPK, ERK1/2, and PI-3K [14]. In addition it was recently demonstrated that Nox2 is phosphorylated by PKC [18]. We decided to evaluate the effect of phosphorylation events on the superoxide overproduction by the D-loop$_{Nox4}$-Nox2 mutant. We used inhibitors of the different kinases involved in the signaling pathway of the oxidase activation by fMLF, ionomycin, PMA and OpZ. PKC phosphorylation events were not involved in the process of superoxide overproduction by the D-loop$_{Nox4}$-Nox2 mutant whatever stimuli used. During OpZ activation, NADPH oxidase activity of the D-loop$_{Nox4}$-Nox2 mutant was less affected by PI3K inhibitors (Wortmaninn and LY-294002) than the WT-Nox2 control cells (50% versus 80% of inhibition). In addition, inhibition of phosphorylation events triggered by the p38 MAPK pathway enhanced oxidase activity of the D-loop$_{Nox4}$-Nox2 mutant activated by OpZ more than the WT-Nox2 cells. PI3K is involved in the OpZ signaling pathway during NADPH oxidase activation and could control phosphorylation of cytosolic factors [70]. PI3K is also involved in the OpZ signaling pathway. PI3K inhibitors could inhibit (less in the D-loop$_{Nox4}$-Nox2 mutant than the WTNox2 cells) secondary phosphorylation events of cytosolic factors possibly triggered by PKD1, PKB, or nonconventional PKC and/or could inhibit the PI3K/p38/Rac pathway involved in the NADPH oxidase activation by OpZ [71,72]. PI3K is also a key regulatory kinase during the first step of signaling events mediated by G protein-coupled receptors (C5a, PAF, fMLF) [70,71]. In fMLF activation, preincubation with PD98059, an ERK1/2 MAPKs inhibitor has a less significant inhibitory effect on NADPH oxidase of the D-loop-Nox2 mutant than on the WT-Nox2 cells as it was found with both PI3K inhibitors after OpZ activation. Moreover, PD-98059 was totally ineffective in inhibiting the oxidase activity of the mutant cells during PMA activation, while the oxidase activity of the WT cells was inhibited by 40%. According to several studies, one of the cascades of phosphorylation triggered by fMLF involved PI3K activation leading to PKC activation (via PDK1) and finally to activated ERK1/2 [16]. PMA can directly activate PKC but can also initiate PKC-dependent Raf/ERK1/2 activation. ERK1/2 MAPKs are responsible for direct phosphorylation of p47^{phox} or p67^{phox} during fMLF, Fcγ receptors, and PMA stimulation [16,26,72]. Then the D-loop$_{Nox4}$-Nox2 mutant seems to be less sensitive to phosphorylation events triggered by ERK1/2 during PMA and fMLF activation. Finally we showed that whatever stimuli used, the oxidase activity in the D-loop$_{Nox4}$-Nox2 PLB-985 was less sensitive to the inhibition of phosphorylation events than the WT PLB-985 cells. This could be explained by a possible change in the mutated Nox2 conformation that modifies the oxidase complex assembly parameters. Perhaps the difference of the D-loop sequence between Nox2 and Nox4 could partially explain the active conformation of Nox4 which is independent of phosphorylated cytosolic factors assembly.

The *in vitro* NADPH oxidase and the INT reductase activities measured after AA activation in the plasma membranes from the mutant PLB-985 and the WT-Nox2 cells were identical even with increasing amounts of human neutrophil cytosol. This demonstrated that the Ca^{2+} influx and/or phosphorylation events related to the overproduce ROS in the D-loop$_{Nox4}$-Nox2 mutant *ex vivo* are not mimicked by AA treatment *in vitro*. Then the *in vitro* oxidase activity was measured in a simplified CFS assay with purified mutant and WT-Nox2 cyt b_{558}, and recombinant p47^{phox}, p67^{phox}, and *Rac* proteins. The same result was obtained after AA activation as in the non purified CFS namely an absence of superoxide overproduction. Nevertheless, the activation by PA reveals the superoxide overproduction of the D-loop$_{Nox4}$-Nox2 cytb_{558}, as if PA triggered a more physiological activation than AA. Fluorescence spectroscopy approaches revealed that anionic amphiphile such as sodium dodecyl sulphate or AA act directly on p47^{phox} to change its conformation [73,74], whereas PA can react directly with cyt b_{558}, in a cytosol-independent manner [75]. In conclusion, PA activation seems to trigger an optimal conformation of the mutant cytb_{558} assembly with cytosolic factors *in vitro*, mimicking what happens in whole D-loop$_{Nox4}$-Nox2 mutant cells.

Finally, we demonstrated that ROS overproduction by the D-loop$_{Nox4}$-Nox2 mutant was responsible for a significantly higher killing activity against attenuated *P. aeruginosa* strain than the WT-Nox2 cell mutant. This is an encouraging result for future protein therapy of CGD because the mutation introduced in Nox2 renders the killing activity more efficient against pathogens. In addition *Pseudomonas* is a catalase positive germ often responsible for infections of CGD patients. However, the mutated or WT-Nox2 PLB-985 cells were much less effective against *S. aureus* ATCC 27217 and *C. albicans* (clinical isolate) than neutrophils, probably more virulent microorganisms than the attenuated strain of *P. aeruginosa* (data not shown). This can be explained by the cyt b_{558} content in the PLB-985 cells which is about ten fold lower than in the human neutrophils [31,51]. We demonstrated that ROS overproduction of the D loop$_{Nox4}$-Nox2 mutant cells has an immediate role in the elimination of bacteria that is more effective than that of the WT-Nox2 ($p<0.05$) in the first period of contact (<30 min), but it also triggers or induces a more active oxidase-independent killing mechanism than that of the WT Nox2 cells ($p<0.01$). This biphasic killing of neutrophils could be related to the previously described dual role of NADPH oxidase in bacterial killing [76]. In addition, XCGD-PLB-985 cells were able to kill bacteria in a NADPH oxidase-independent way only after a 30-min period of incubation. This highlights that the NADPH oxidase-dependent killing takes place in the early phase of contact (<30 min). In conclusion, early ROS overproduction by the NADPH oxidase in neutrophils is the essential starting point event that controls the efficacy of the killing of bacteria.

The next step will be to produce *ex vivo*, in yeast [77], the modified Nox2 protein including the D-loopNox4 and/or the R199Q mutation [51] to obtain a superactive protein used for structural and functional studies. Preliminary results obtained recently support the concept of cell-free expression technology for producing recombinant

proteoliposomes and their use for functional and structural studies or protein therapy by complementing Nox2-deficient cells [78].

Acknowledgments

The authors are grateful to Pr. Mary C. Dinauer for the generous gift of X-CGD PLB-985 cells. The antibodies 449 and 48 were generous gifts from Pr. D. Roos. We are so grateful to Cécile Martel, and Michelle Mollin, for their enthusiasm at work at the Centre Diagnostic et Recherche CGD. Special thanks are extended to Lila Laval for her excellent secretarial work and to Linda Northrup for editing the manuscript.

Supported by grants from the US Immunodeficiency Network (USIDNET) and the Primary Immunodeficiency Disease Consortium's National Institutes of Health contract no. N01-AI-30070 supported this work. It was also supported by grants from the Université Joseph Fourier and the Faculté de Médecine; the Ministère de l'Education et de la Recherche; MENRT; and the Direction de la Recherche Régionale Clinique, DRRC.

References

[1] A.W. Segal, How neutrophils kill microbes, Annu. Rev. Immunol. 23 (2008) 197–223.
[2] M.J. Stasia, X.J. Li, Genetics and immunopathology of chronic granulomatous disease, Semin. Immunopathol. 30 (2008) 209–235.
[3] P.V. Vignais, The superoxide-generated NADPH oxidase: structural aspects and activation mechanism, Cell. Mol. Life Sci. 59 (2002) 1428–1459.
[4] A.W. Segal, I. West, F. Wientjes, J.H. Nugent, A.J. Chavan, B. Haley, R.C. Garcia, H. Rosen, G. Scrace, Cytochrome b-245 is a flavocytochrome containing FAD and the NADPH-binding site of the microbicidal oxidase of phagocytes, Biochem. J. 284 (Pt 3) (1992) 781–788.
[5] D. Rotrosen, C.L. Yeung, T.L. Leto, H.L. Malech, C.H. Kwong, Cytochrome b558: the flavin-binding component of the phagocyte NADPH oxidase, Science 256 (1992) 1459–1462.
[6] H. Sumimoto, N. Sakamoto, M. Nozaki, Y. Sakaki, K. Takeshige, S. Minakami, Cytochrome b558, a component of the phagocyte NADPH oxidase, is a flavoprotein, Biochem. Biophys. Res. Commun. 186 (1992) 1368–1375.
[7] J.D. Lambeth, T. Kawahara, B. Diebold, Regulation of Nox and Duox enzymatic activity and expression, Free Radic. Biol. Med. 43 (2007) 319–331.
[8] K. Bedard, K.H. Krause, The NOX family of ROS-generating NADPH oxidases: physiology and pathophysiology, Physiol. Rev. 87 (2007) 245–313.
[9] W.M. Nauseef, Nox enzymes in immune cells, Semin. Immunopathol. 30 (2008) 195–208.
[10] R.A. Clark, B.D. Volpp, K.G. Leidal, W.M. Nauseef, Two cytosolic components of the human neutrophil respiratory burst oxidase translocate to the plasma membrane during cell activation, J. Clin. Invest. 85 (1990) 714–721.
[11] M.T. Quinn, T. Evans, L.R. Loetterle, A.J. Jesaitis, G.M. Bokoch, Translocation of Rac correlates with NADPH oxidase activation: evidence for equimolar translocation of oxidase components, J. Biol. Chem. 268 (1993) 20983–20987.
[12] S. Dusi, F. Rossi, Activation of NADPH oxidase of human neutrophils involves the phosphorylation and the translocation of cytosolic p67phox, Biochem. J. 296 (1993) 367–371.
[13] A.P. Bouin, N. Grandvaux, P.V. Vignais, A. Fuchs, p40(phox) is phosphorylated on threonine 154 and serine 315 during activation of the phagocyte NADPH oxidase. Implication of a protein kinase c-type kinase in the phosphorylation process, J. Biol. Chem. 273 (1998) 30097–30103.
[14] J. El-Benna, L.P. Faus, J.L. Johnson, B.M. Babior, Phosphorylation of the respiratory burst oxidase subunit p47phox as determined by two-dimensional phosphopeptide mapping. Phosphorylation by protein kinase C, protein kinase A, and a mitogen-activated protein kinase, J. Biol. Chem. 271 (1996) 6374–6378.
[15] T. Ago, H. Nunoi, T. Ito, H. Sumimoto, Mechanism for phosphorylation- induced activation of the phagocyte NADPH oxidase protein p47(phox). Triple replacement of serines 303, 304, and 328 with aspartates disrupts the SH3 domain-mediated intramolecular interaction in p47phox, thereby activating the oxidase, J. Biol. Chem. 274 (1999) 33644–33653.
[16] R. Lofgren, L. Serrander, M. Forsberg, A. Wilsson, A. Wasteson, O. Stendahl, CR3, FcgammaRIIA and FcgammaRIIIB induce activation of the respiratory burst in human neutrophils: the role of intracellular Ca(2+), phospholipase D and tyrosine phosphorylation, Biochim. Biophys. Acta 1452 (1999) 46–59.
[17] D.S. Regier, D.G. Greene, S. Sergeant, A.J. Jesaitis, L.C. McPhail, Phosphorylation of p22phox is mediated by phospholipase D-dependent and -independent mechanisms. Correlation of NADPH oxidase activity and p22phox phosphorylation, J. Biol. Chem. 275 (2000) 28406–28412.
[18] H. Raad, M.H. Paclet, T. Boussetta, Y. Kroviarski, F. Morel, M.T. Quinn, M.A. Gougerot- Pocidalo, P.M. Dang, J. El-Benna, Regulation of the phagocyte NADPH oxidase activity: phosphorylation of gp91phox/NOX2 by protein kinase C enhances its diaphorase activity and binding to Rac2, p67phox, and p47phox, FASEB J. 23 (2009) 1011–1022.
[19] C. Massenet, S. Chenavas, C. Cohen-Addad, M.C. Dagher, G. Brandolin, E. Pebay-Peyroula, F. Fieschi, Effects of p47phox C terminus phosphorylations on binding interactions with p40phox and p67phox. Structural and functional comparison of p40phox and p67phox SH3 domains, J. Biol. Chem. 280 (2005) 13752–13761.
[20] J. Marcoux, P. Man, M. Castellan, C. Vivès, E. Forest, F. Fieschi, Conformational changes in (p47)phox upon activation highlighted by mass spectrometry coupled to hydrogen/deuterium exchange and limited proteolysis, FEBS Lett. 583 (2009) 835–840.
[21] I. Nobuhisa, R. Takeya, K. Ogura, N. Ueno, D. Kohda, F. Inagaki, H. Sumimoto, Activation of the superoxide-producing phagocyte NADPH oxidase requires cooperation between the tandem SH3 domains of p47phox in recognition of a polyproline type II helix and an adjacent alpha-helix of p22phox, Biochem. J. 396 (2006) 183–192.
[22] A. Fontayne, P.M.C. Dang, M.A. Gougerot-Pocidalo, J. El Benna, Phosphorylation of p47phox sites by PKC α, βII, δ, and ζ: effect on binding to p22phox and on NADPH oxidase activation, Biochemistry 41 (2002) 7743–7750.
[23] P.G. Heyworth, J.T. Curnutte, W.M. Nauseef, B.D. Volpp, D.W. Pearson, H. Rosen, R.A. Clark, Neutrophil nicotinamide adenine dinucleotide phosphate oxidase assembly. Translocation of p47-phox and p67-phox requires interaction between p47-phox and cytochrome b558, J. Clin. Invest. 87 (1991) 352–356.
[24] R. Nakamura, H. Sumimoto, K. Mizuki, K. Hata, T. Ago, S. Kitajima, K. Takeshige, Y. Sakaki, T. Ito, The PC motif: a novel and evolutionary conserved sequence involved in interaction between p40phox and p67phox, SH3 domain-containing cytosolic factors of the phagocyte NADPH oxidase, Eur. J. Biochem. 251 (1998) 583–589.
[25] K. Lapouge, S.J. Smith, Y. Groemping, K. Rittinger, Architecture of the p40-p47-p67phox complex in the resting state of the NADPH oxidase: a central role for p67phox, J. Biol. Chem. 277 (2002) 10121–10128.
[26] L.V. Forbes, S.J. Moss, A.W. Segal, Phosphorylation of p67phox in the neutrophil occurs in the cytosol and is independent of p47phox, FEBS Lett. 449 (1999) 225–229.
[27] P.M. Dang, F. Morel, M.A. Gougerot-Pocidalo, J. El Benna, Phosphorylation of the NADPH oxidase component p67phox by ERK2 and P38MAPK: selectivity of phosphorylated sites and existence of an intramolecular regulatory domain in the tetratricopeptide-rich region, Biochemistry 42 (2003) 4520–4526.
[28] Y. Nisimoto, S. Motalebi, C.H. Han, J.D. Lambeth, The p67(phox) activation domain regulates electron flow from NADPH to flavin in flavocytochrome b(558), J. Biol. Chem. 274 (1999) 22999–23005.
[29] M.H. Paclet, A.W. Coleman, S. Vergnaud, F. Morel, P67-phox-mediated NADPH oxidase assembly: imaging of cytochrome b558 liposomes by atomic force microscopy, Biochemistry 39 (2000) 9302–9310.
[30] P.M. Dang, A.R. Cross, B.M. Babior, Assembly of the neutrophil respiratory burst oxidase: a direct interaction between p67phox and cytochrome b558, Proc. Natl. Acad. Sci. U. S. A. 98 (2001) 3001–3005.
[31] X.J. Li, F. Fieschi, M.H. Paclet, D. Grunwald, Y. Campion, P. Gaudin, F. Morel, M.J. Stasia, Leu505 of Nox2 is crucial for optimal p67phox-dependent activation of the flavocytochrome b558 during phagocytic NADPH oxidase assembly, J. Leukoc. Biol. 81 (2007) 238–249.
[32] R. Sarfstein, Y. Gorzalczany, A. Mizrahi, Y. Berdichevsky, S. Molshanski-Mor, C. Weinbaum, M. Hirshberg, M.C. Dagher, E. Pick, Dual role of Rac in the assembly of NADPH oxidase, tethering to the membrane and activation of p67phox: a study based on mutagenesis of p67phox-Rac1 chimeras, J. Biol. Chem. 279 (2004) 16007–16016.
[33] J. El-Benna, P.M. Dang, M. Gaudry, M. Fay, F. Morel, J. Hakim, M.A. Gougerot-Pocidalo, Phosphorylation of the respiratory burst oxidase subunit p67phox during human neutrophil activation. Regulation by protein kinase C-dependent and independent pathways, J. Biol. Chem. 272 (1997) 17204–17208.
[34] F.R. Sheppard, M.R. Kelher, E.E. Moore, N.J. McLaughlin, A. Banerjee, C.C. Silliman, Structural organization of the neutrophil NADPH oxidase: phosphorylation and translocation during priming and activation, J. Leukoc. Biol. 78 (2005) 1025–1042.
[35] E.P. Reeves, L.V. Dekker, L.V. Forbes, F.B. Wientjes, A. Grogan, D.J. Pappin, W. Segal, Direct interaction between p47phox and protein kinase C: evidence for targeting of protein kinase C by p47phox in neutrophils, Biochem. J. 344 (Pt 3) (1999) 859–866.
[36] G.E. Brown, M.Q. Stewart, S.A. Bissonnette, A.E. Elia, E. Wilker, M.B. Yaffe, Distinct ligand-dependent roles for p38 MAPK in priming and activation of the neutrophil NADPH oxidase, J. Biol. Chem. 279 (2004) 27059–27068.
[37] L.W. Chen, M.W. Lin, C.M. Hsu, Different pathways leading to activation of extracellular signal-regulated kinase and p38 MAP kinase by formyl-methionyl-leucyl- phenylalanine or platelet activating factor in human neutrophils, J. Biomed. Sci. 12 (2005) 311–319.
[38] P.M. Dang, A. Stensballe, T. Boussette, H. Raad, C. Dewas, Y. Kroviarski, G. Hayem, O.N. Jensen, M.A. Gougerot-Pocidalo, J. El Benna, A specific p47phox-serine phosphorylated by convergent MAPKs mediates neutrophil NADPH oxidase priming at inflammatory sites, J. Clin. Invest. 116 (2006) 2033–2043.
[39] J.A. Le Good, W.H. Ziegler, D.B. Parekh, D.R. Alessi, P. Cohen, P.J. Parker, Protein kinase C isotypes controlled by phosphoinositide 3-kinase through the protein kinase PDK1, Science 281 (1998) 2042–2045.
[40] T. Ago, F. Kuribayashi, H. Hiroaki, R. Takeya, T. Ito, D. Kohda, H. Sumimoto, Phosphorylation of p47phox directs phox homology domain from SH3 domain toward phsophoinositides, leading to phagocyte NADPH oxidase activation, Proc. Natl. Acad. Sci. U. S. A. 100 (2003) 4474–4479.
[41] W. Tian, X.J. Li, N.D. Stull, W. Ming, C.I. Suh, S.A. Bissonnette, M.B. Yaffe, S. Grinstein, S.J. Atkinson, M.C. Dinauer, Fc{gamma}R-stimulated activation of the NADPH oxidase: Phosphoinositide binding protein p40phox regulates NADPH oxidase activity after enzyme assembly on the phagosome, Blood 112 (2008) 3867–3877.

[42] R. Dana, T.L. Leto, H.L. Malech, R. Levy, Essential requirement of cytosolic phospholipase A2 for activation of the phagocyte NADPH oxidase, J. Biol. Chem. 273 (1998) 441–445.
[43] Z. Shmelzer, M. Karter, M. Eisenstein, T.L. Leto, N. Hadad, D. Ben-Menahem, D. Gitler, S. Banani, B. Wolach, M. Rotem, R. Levy, Cystosolic phospholipase A2alpha is targeted to p47phox-PX domain of the assembled NADPH oxidase via a novel binding site in its C2 domain, J. Biol. Chem. 283 (2008) 31898–31908.
[44] S. Bréchard, E.J. Tschirhart, Regulation of superoxide production in neutrophils: role of calcium influx, J. Leukoc. Biol. 84 (2008) 1223–1237.
[45] R. Foyouzi-Youssefi, F. Petersson, D.P. Lew, K.H. Krause, O. Nüsse, Chemoattractant- induced respiratory burst: increases in cytosolic Ca2+ concentrations are essential and synergize with a kinetically distinct second signal, Biochem. J. 15 (1997) 709–718.
[46] S. Dewitt, I. Laffafian, M.B. Hallett, Phagosomal oxidative activity during beta2 integrin (CR3)-mediated phagocytosis by neutrophils is triggered by a non-restricted Ca2+ signal: Ca2+ controls time not space, J. Cell Sci. 116 (2003) 2857–2865.
[47] H.M. Korchak, L.B. Dorsey, H. Li, D. Mackie, L.E. Kilpatrick, Selective roles for alpha-PKC in positive signaling for O-(2) generation and calcium mobilization but not elastase release in differentiated HL60 cells, Biochim. Biophys. Acta 1773 (2007) 440–449.
[48] C.C. Leslie, Properties and regulation of cytosolic phospholipase A2, J. Biol. Chem. 272 (1997) 16709–16712.
[49] P.G. Heyworth, J.A. Badwey, Continuous phosphorylation of both the 47 and the 49 kDa proteins occurs during superoxide production by neutrophils, Biochim. Biophys. Acta 1052 (1990) 299–305.
[50] T.E. DeCoursey, E. Ligeti, Regulation and termination of NADPH oxidase activity, Cell. Mol. Life Sci. 62 (2005) 2173–2193.
[51] X.J. Li, D. Grunwald, J. Mathieu, F. Morel, M.J. Stasia, Crucial role of two potential cytosolic regions of Nox2, 191TSSTKTIRRS200 and 484DESQANHFAVHH-DEEKD500, on NADPH oxidase activation, J. Biol. Chem. 280 (2005) 4962–14973.
[52] L. Zhen, A.A. King, Y. Xiao, S.J. Chanock, S.H. Orkin, M.C. Dinauer, Gene targeting of X chromosome-linked chronic granulomatous disease locus in a human myeloid leukaemia cell line and rescue by expression of recombinant gp91phox, Proc. Natl. Acad. Sci. U. S. A. 90 (1993) 9832–9836.
[53] A. Boyum, Separation of leukocytes from blood and bone marrow. Introduction, Scand. J. Clin. Lab. Invest. Suppl. 97 (1968) 77–89.
[54] C.I. Lord, M.H. Riesselman, J.M. Gripentrog, J.B. Burritt, A.J. Jesaitis, R.M. Taylor, Single-step immunoaffinity purification and functional reconstitution of human phagocyte flavocytochrome b, J. Immunol. Methods 329 (2008) 201–217.
[55] A. Abo, A. Boyhan, I. West, A.J. Thrasher, A.W. Segal, Reconstitution of neutrophil NADPH oxidase activity in the cell-free system by four components: p67-phox, p47-phox, p21rac1, and cytochrome b-245, J. Biol. Chem. 267 (1992) 16767–16770.
[56] S. Vergnaud, M.H. Paclet, J. El Benna, M.A. Pocidalo, F. Morel, Complementation of NADPH oxidase in p67-phox-deficient CGD patients p67- phox/p40-phox interaction, Eur. J. Biochem. 267 (2000) 1059–1067.
[57] C. Dahlgren, A. Karlsson, Respiratory burst in human neutrophils, J. Immunol. Methods 232 (1999) 3–14.
[58] C. Bionda, X.J. Li, R. van Bruggen, M. Eppink, D. Roos, F. Morel, M.J. Stasia, Functional analysis of two-amino acid substitutions in gp91 phox in a patient with X-linked flavocytochrome b558-positive chronic granulomatous disease by means of transgenic PLB- 985 cells, Hum. Genet. 115 (2004) 418–427.
[59] L. Cohen-Tanugi, F. Morel, M.C. Pilloud-Dagher, J.M. Seigneurin, P. Francois, M. Bost, P.V. Vignais, Activation of O2(-)-generating oxidase in an heterologous cell-free-system derived from Epstein-Barr-virus-transformed human B lymphocytes and bovine neutrophils. Application to the study of defects in cytosolic factors in chronic granulomatous disease, Eur. J. Biochem. 202 (1991) 649–655.
[60] A.R. Cross, J.L. Yarchover, J.T. Curnutte, The superoxide-generating system of human neutrophils possesses a novel diaphorase activity. Evidence for distinct regulation of electron flow within NADPH oxidase by p67-phox and p47-phox, J. Biol. Chem. 269 (1994) 21448–21454.
[61] R.M. Taylor, C.I. Lord, M.H. Riesselman, J.M. Gripentrog, T.L. Leto, L.D. McPhail, Y. Berdichevsky, E. Pick, A.J. Jesaitis, Characterization of surface structure and p47phox SH3 domain-mediated conformational changes for human neutrophil flavocytochrome *b*, Biochemistry 46 (2007) 14291–14304.
[62] D. Dacheux, I. Attree, C. Schneider, B. Toussaint, Cell death of human polymorphonuclear neutrophils induced by a *Pseudomonas aeruginosa* cystic fibrosis isolate requires a functional type III secretion system, Infect. Immun. 67 (1999) 6164–6167.
[63] E. Decleva, R. Menegazzi, S. Busetto, P. Patriarca, P. Dri, Common methodology is inadequate for studies on the microbicidal activity of neutrophils, J. Leukoc. Biol. 79 (2006) 87–94.
[64] M.M. Bradford, A rapid and sensitive method for the quantitation of microgram quantities of protein utilizing the principle of protein-dye binding, Anal. Biochem. 72 (1976) 248–254.
[65] P.K. Smith, R.I. Krohn, G.T. Hermanson, A.K. Mallia, F.H. Gartner, M.D. Provenzano, E.K. Fujimoto, N.M. Goeke, B.J. Olson, D.C. Klenk, Measurement of protein using bicinchoninic acid, Anal. Biochem. 150 (1985) 76–85.
[66] X.J. Li, W. Tian, N.D. Stull, S. Grinstein, S. Atkinson, M.C. Dinauer, A fluorescently tagged C-terminal fragment of p47phox detects NADPH oxidase dynamics during phagocytosis, Mol. Biol. Cell 20 (2009) 1520–1532.
[67] E. Pedruzzi, M. Fay, C. Elbim, M. Gaudry, M.A. Gougerot-Pocidalo, Differentiation of PLB-985 myeloid cells into mature neutrophils, shown by degranulation of terminally differentiated compartments in response to N-formyl peptide and priming of superoxide anion production by granulocyte-macrophage colony-stimulating factor, Br. J. Haematol. 117 (2002) 719–726.
[68] K.A. Tucker, M.B. Lilly, L. Jr, T.A. Rado Heck, Characterization of a new human diploid myeloid leukemia cell line (PLB-985) with granulocytic and monocytic differentiating capacity, Blood 70 (1987) 372–378.
[69] C. Pivot-Pajot, F.C. Chouinard, M.A. El Azreq, D. Harbour, S.G. Bourgoin, Characterisation of degranulation and phagocytic capacity of a human neutrophilic cellular model, PLB-985 cells, Immunobiology 215 (2010) 38–52.
[70] P.T. Hawkins, K. Davidson, L.R. Stephens, The role of PI3Ks in the regulation of the neutrophil NADPH oxidase. Biochem. Soc. Symp. 59-67.
[71] M.J. Rabiet, E. Huet, F. Boulay, The N-formyl peptide receptors and the anaphylatoxin C5a receptors: and overview, Biochimie 89 (2007) 1089–1106.
[72] C. Dewas, M. Fay, M.A. Gougerot-¯Pocidalo, J. El-Benna, The mitogen-activated protein kinase extracellular signal-regulated kinase 1/2 pathway is involved in formyl- methionyl-leucyl-phenylalanine-induced p47phox phosphorylation in human neutrophils, J. Immunol. 165 (2000) 5238–5244.
[73] S.D. Swain, S.L. Helgerson, A.R. Davis, L.K. Nelson, M.T. Quinn, Analysis of activation- induced conformational changes in p47phox using tryptophan fluorescence spectroscopy, J. Biol. Chem. 272 (1997) 29502–29510.
[74] H.S. Park, J.W. Park, Fluorescent labeling of the leukocyte NADPH oxidase subunit p47(phox): evidence for amphiphile-induced conformational changes, Arch. Biochem. Biophys. 360 (1998) 165–172.
[75] V. Koshkin, E. Pick, Generation of superoxide by purified and relipidated cytochrome b559 in the absence of cytosolic activators, FEBS Lett. 327 (1993) 57–62.
[76] B.K. Rada, M. Geiszt, K. Káldi, C. Timár, E. Ligeti, Dual role of phagocytic NADPH oxidase in bacterial killing, Blood 104 (2004) 2947–2953.
[77] M.A. Ostuni, L.B. Lamanuzzi, T. Bizouarn, M.C. Dagher, L. Baciou, Expression of functional mammal flavocytochrome b(558) in yeast: Comparison with improved insect cell system, Biochim. Biophys. Acta 1798 (2010) 1179–1188.
[78] B. Marques, L. Liguori, M.H. Paclet, A. Villegas-Mendez, R. Rothe, F. Morel, J.L. Lenormand, Liposome-mediated cellular delivery of active gp91(phox), PLoS One 2 (2007) e856.